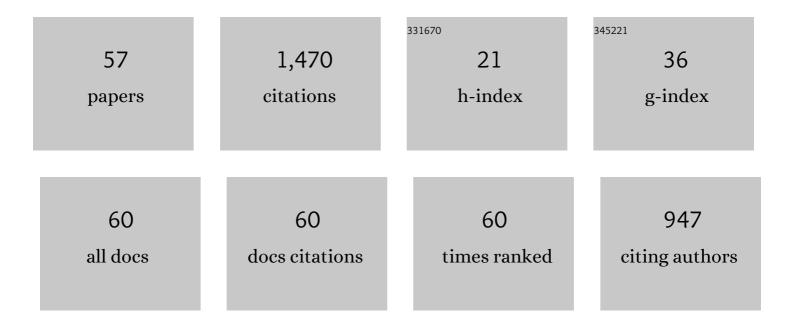
Xiao-Ming Duan

List of Publications by Year in descending order

Source: https://exaly.com/author-pdf/6570052/publications.pdf Version: 2024-02-01



XIAO-MINC DUAN

#	Article	IF	CITATIONS
1	Influence of sintering temperature on the crystallization and mechanical properties of BNâ€MAS composites. Journal of the American Ceramic Society, 2022, 105, 3590-3600.	3.8	5
2	Improved mechanical properties and directional heat transfer performance of h-BN matrix multilayer composites with alternately stacked untextured/textured layers. Ceramics International, 2022, 48, 13563-13571.	4.8	3
3	Texture and anisotropy of hot-pressed h-BN matrix composite ceramics with in situ formed YAG. Journal of Advanced Ceramics, 2022, 11, 532-544.	17.4	17
4	3D Printing of Damageâ€ŧolerant Martian Regolith Simulantâ€based Geopolymer Composites. Additive Manufacturing, 2022, 58, 103025.	3.0	6
5	Improvement of grain size and crystallization degree of LPSed h-BN composite ceramics by amorphization/nanocrystallization of raw h-BN powders. Journal of Alloys and Compounds, 2021, 852, 156765.	5.5	7
6	Cyclic thermal shock resistance of h-BN composite ceramics with La2O3–Al2O3–SiO2 addition. Ceramics International, 2021, 47, 73-79.	4.8	10
7	Microstructural evolution of h-BN matrix composite ceramics with La-Al-Si-O glass phase during hot-pressed sintering. Journal of Advanced Ceramics, 2021, 10, 493-501.	17.4	22
8	Effect of Re2O3–MgO additives on the microstructure evolution and properties of β-Si3N4 ceramics. Ceramics International, 2021, 47, 22073-22079.	4.8	11
9	Formation of SiC whiskers/leucite-based ceramic composites from low temperature hardening geopolymer. Ceramics International, 2021, 47, 17930-17938.	4.8	10
10	On the formation mechanisms and properties of MAX phases: A review. Journal of the European Ceramic Society, 2021, 41, 3851-3878.	5.7	97
11	3D-printing of architectured short carbon fiber-geopolymer composite. Composites Part B: Engineering, 2021, 226, 109348.	12.0	57
12	Effects of sintering temperature on the microstructure and properties of h-BN ceramics with MAS as liquid sintering aid. Ceramics International, 2020, 46, 1076-1082.	4.8	7
13	Microstructural evolution and mechanical properties of h-BN composite ceramics with Y2O3–AlN addition by liquid-phase sintering. Rare Metals, 2020, 39, 555-561.	7.1	12
14	Immobilization behavior of Sr in geopolymer and its ceramic product. Journal of the American Ceramic Society, 2020, 103, 1372-1384.	3.8	24
15	Insight into hexacelsian-to-celsian transformation in hot-pressed BN/BAS composites. Journal of the European Ceramic Society, 2020, 40, 1773-1778.	5.7	12
16	Grain-orientation dependence of the anisotropic thermal shock performance of hexagonal boron nitride ceramics. Scripta Materialia, 2020, 178, 402-407.	5.2	9
17	The effects of holding time on grain size, orientation degree and properties of h-BN matrix textured ceramics. Materials Chemistry and Physics, 2020, 248, 122916.	4.0	12
18	Preparation of highly oriented h-BN based textured ceramics via grain rearrangement under DLP printing and low-pressure sintering. Materials Letters, 2020, 268, 127584.	2.6	5

XIAO-MING DUAN

#	Article	IF	CITATIONS
19	SnO2 nanoparticles anchored on chlorinated graphene formed directly on Cu foil as binder-free anode materials for lithium-ion batteries. Applied Surface Science, 2020, 519, 146190.	6.1	11
20	Microstructure and room/elevated-temperature mechanical properties of hot-pressed h-BN composite ceramics with La2O3-Al2O3-SiO2 addition. Journal of the European Ceramic Society, 2020, 40, 2260-2267.	5.7	5
21	Microstructure evolution and grain growth mechanisms of h-BN ceramics during hot-pressing. Journal of the European Ceramic Society, 2020, 40, 2268-2278.	5.7	21
22	From bulk to porous structures: Tailoring monoclinic SrAl ₂ Si ₂ O ₈ ceramic by geopolymer precursor technique. Journal of the American Ceramic Society, 2020, 103, 4957-4968.	3.8	10
23	Preparation and anisotropic properties of textured structural ceramics: A review. Journal of Advanced Ceramics, 2019, 8, 289-332.	17.4	107
24	In situ ZrC/Si-B-C-N monoliths prepared by sol-gel and reactive hot-pressing: Processing, microstructure, mechanical properties and oxidation behavior. Journal of Alloys and Compounds, 2019, 811, 151687.	5.5	3
25	Effect of ball milling treatment on the microstructures and properties of Cr2AlC powders and hot pressed bulk ceramics. Journal of the European Ceramic Society, 2019, 39, 5140-5148.	5.7	9
26	Safe trapping of cesium into doping-enhanced pollucite structure by geopolymer precursor technique. Journal of Hazardous Materials, 2019, 367, 577-588.	12.4	43
27	MAS-content dependence of the texture and fracture behavior of h-BN-MAS composite ceramics. Ceramics International, 2019, 45, 18536-18542.	4.8	4
28	Thermal properties and thermal shock resistance of BAS-BN composite ceramics. Ceramics International, 2019, 45, 8181-8187.	4.8	27
29	Anisotropic properties of textured h-BN matrix ceramics prepared using 3Y2O3-5Al2O3(-4MgO) as sintering additives. Journal of the European Ceramic Society, 2019, 39, 1788-1795.	5.7	14
30	Anisotropies in structure and properties of hot-press sintered h-BN-MAS composite ceramics: Effects of raw h-BN particle size. Journal of the European Ceramic Society, 2019, 39, 539-546.	5.7	34
31	Effect of the starting AlN content on the phase formation and property of the novel in-situ fabricated X-SiAlON/BN composites. Journal of the European Ceramic Society, 2019, 39, 934-943.	5.7	9
32	Role of boron addition on phase composition, microstructural evolution and mechanical properties of nanocrystalline SiBCN monoliths. Journal of the European Ceramic Society, 2018, 38, 1179-1189.	5.7	13
33	Ablation behavior and mechanism of boron nitride - magnesium aluminum silicate ceramic composites in an oxyacetylene combustion flame. Ceramics International, 2018, 44, 1518-1525.	4.8	4
34	In situ processing of MWCNTs/leucite composites through geopolymer precursor. Journal of the European Ceramic Society, 2017, 37, 2219-2226.	5.7	41
35	Manufacturing of high volume fraction of Ti 3 AlC 2 -Ti 2 AlC metallic ceramics as nano-multilayered structures through high energy milling, hot pressing and liquid phase sintering. Materials Characterization, 2017, 128, 176-183.	4.4	4
36	Effects of boron addition on the high temperature oxidation resistance of dense sSiBCN monoliths at 1500 °C. Corrosion Science, 2017, 126, 10-25.	6.6	33

XIAO-MING DUAN

#	Article	IF	CITATIONS
37	High-temperature oxidation behavior of dense SiBCN monoliths: Carbon-content dependent oxidation structure, kinetics and mechanisms. Corrosion Science, 2017, 124, 103-120.	6.6	30
38	Effect of the BN content on the thermal shock resistance and properties of BN/SiO ₂ composites fabricated from mechanically alloyed SiBON powders. RSC Advances, 2017, 7, 48994-49003.	3.6	18
39	Review on the properties of hexagonal boron nitride matrix composite ceramics. Journal of the European Ceramic Society, 2016, 36, 3725-3737.	5.7	107
40	Crystallization kinetics and microstructure evolution of reduced graphene oxide/geopolymer composites. Journal of the European Ceramic Society, 2016, 36, 2601-2609.	5.7	24
41	Microstructure and erosion resistance of in-situ SiAlON reinforced BN-SiO2 composite ceramics. Journal Wuhan University of Technology, Materials Science Edition, 2016, 31, 315-320.	1.0	7
42	Influence of hot-press sintering parameters on microstructures and mechanical properties of h-BN ceramics. Journal of Alloys and Compounds, 2016, 684, 474-480.	5.5	31
43	Influence of sintering pressure on the crystallization and mechanical properties of BN-MAS composite ceramics. Journal of Materials Science, 2016, 51, 2292-2298.	3.7	20
44	SiC fiber reinforced geopolymer composites, part 1: Short SiC fiber. Ceramics International, 2016, 42, 5345-5352.	4.8	43
45	Inhibiting crystallization mechanism of h -BN on α-cordierite in BN-MAS composites. Journal of the European Ceramic Society, 2016, 36, 905-909.	5.7	22
46	Synthesis of high-purity, isotropic or textured Cr 2 AlC bulk ceramics by spark plasma sintering of pressure-less sintered powders. Journal of the European Ceramic Society, 2015, 35, 1393-1400.	5.7	64
47	A novel BN–MAS system composite ceramics with greatly improved mechanical properties prepared by low temperature hot-pressing. Materials Science & Engineering A: Structural Materials: Properties, Microstructure and Processing, 2015, 633, 194-199.	5.6	44
48	Preparation of fully stabilized cubic-leucite composite through heat-treating Cs-substituted K-geopolymer composite at high temperatures. Composites Science and Technology, 2015, 107, 44-53.	7.8	21
49	Ablation mechanism and properties of in-situ SiAlON reinforced BN–SiO2 ceramic composite under an oxyacetylene torch environment. Ceramics International, 2014, 40, 11149-11155.	4.8	13
50	lon sputtering erosion mechanisms of h-BN composite ceramics with textured microstructures. Journal of Alloys and Compounds, 2014, 613, 1-7.	5.5	14
51	Anisotropic mechanical properties and fracture mechanisms of textured h-BN composite ceramics. Materials Science & Engineering A: Structural Materials: Properties, Microstructure and Processing, 2014, 607, 38-43.	5.6	63
52	Mechanical properties and plasma erosion resistance of BNp/Al2O3-SiO2 composite ceramics. Journal of Central South University, 2013, 20, 1462-1468.	3.0	10
53	Effect of sintering pressure on the texture of hot-press sintered hexagonal boron nitride composite ceramics. Scripta Materialia, 2013, 68, 104-107.	5.2	68
54	Study on the plasma erosion resistance of ZrO2p(3Y)/BN–SiO2 composite ceramics. Composites Part B: Engineering, 2013, 46, 130-134.	12.0	11

#	Article	IF	CITATIONS
55	Progress of a novel non-oxide Si-B-C-N ceramic and its matrix composites. Journal of Advanced Ceramics, 2012, 1, 157-178.	17.4	81
56	Effect of Preforming Process and Starting Fused SiO ₂ Particle Size on Microstructure and Mechanical Properties of Pressurelessly Sintered BN _p /SiO ₂ Ceramic Composites. Journal of the American Ceramic Society, 2011, 94, 3552-3560.	3.8	56
57	Preparation and mechanical performance of SiC w /geopolymer composites through direct ink writing. Journal of the American Ceramic Society, 0, , .	3.8	5